THE ASTROPHYSICAL JOURNAL, 422:783–790, 1994 February 20

GD 323: NEW OBSERVATIONS AND ANALYSIS OF THE PROTOTYPE DAB WHITE DWARF

D. KOESTER[1]
Department of Physics and Astronomy, Louisiana State University, Baton Rouge, LA 70803-4001
JAMES LIEBERT[2]
Steward Observatory, University of Arizona, Tucson, AZ 85721
AND
REX A. SAFFER
Space Telescope Science Institute,[3] 3700 San Martin Drive, Baltimore, MD 21218
Received 1993 June 30; accepted 1993 August 27

ABSTRACT

In this paper we present new spectroscopic observations of very high quality of the hybrid DAB white dwarf GD 323. GD 323 shows both hydrogen and helium lines and is located at an effective temperature ($\approx$28,750 K), which places it at the hot end of the DB sequence just below the empirical DB gap. With recent results for the related object G104−7 in mind (Holberg et al. 1990), we first discount the possibility of variability. Repeated spectra obtained with similar instrument parameters reveal little evidence of spectroscopic variability on time scales from hours to a decade.

We explore four different scenarios in our attempt to understand the energy distribution from the UV to the red and the optical spectrum: a mixed H/He atmosphere, a binary DA + DB, a simple spot model of hydrogen and helium-rich areas on the surface, and a stratified H/He atmosphere in diffusion equilibrium. None of the models studied allows a completely satisfactory fit to all observations; the scenario that seems most promising is that of a statified atmosphere. However, with standard input physics, even this cannot explain the detailed line profiles observed.

Subject headings: stars: atmospheres — stars: individual (GD 323) — white dwarfs

1. INTRODUCTION

GD 323 was originally classified DBp (peculiar) by Greenstein (1969), who noticed weak He lines in the optical spectrum. It was later found to show also broad, shallow hydrogen lines, and thus was reclassified DAB by Oke, Weidemann, & Koester (1984) and simultaneously by Liebert et al. (1984), LWSW). Using ultraviolet (*IUE*) and optical spectra, LWSW demonstrated that the object has an energy distribution from the UV to the red characteristic of a helium-dominated atmosphere around 30,000 K, but with lines of H and He much too weak for this temperature. They analyzed the spectra using homogeneous model atmospheres but were unable to find a consistent fit. After a discussion of several alternative hypotheses (interstellar reddening, rotation, accretion disks, binary system), they concluded that the only remaining viable hypothesis was that of a stratified atmosphere, which could not be tested at that time due to the lack of detailed models.

Since that time, this gap has been filled with the calculation of model atmospheres in diffusion equilibrium, with a hydrogen layer flating on top of the underlying helium envelope and a realistic transition layer (Price & Shipman 1985; Jordan & Koester 1986; Koester 1989; Vennes et al. 1989; Vennes & Fontaine 1992). Preliminary applications of these new models seemed to indicate that it is possible to fit the energy distribution and optical spectra with such models (Koester 1989, 1991).

GD 323, the prototype of the DAB class, is not unique. A possible second object of this class, G104−27, was discussed by Holbert, Kidder, & Wesemael (1990), although this case remains somewhat doubtful, since the helium lines were not seen in more recent observations (Kidder et al. 1992). More recently, two more DAB (MCT 0453−2933 and MCT 0128−3846) were discovered in the course of the southern hemisphere Montreal-Cambridge-Tololo Survey of blue subluminous stars (Wesemael et al. 1993). These two objects showed similar discrepancies between the energy distribution and optical spectra as found in the prototype GD 323. A preliminary analysis by Wesemael et al. (1993) using homogeneous and stratified model atmospheres found better agreement but no completely satisfactory fit with the latter assumption.

Although GD 323 did not show any evidence for variations on short timescales in the fast photometry of Robinson & Winget (1983), the contradictory observations of the related object G104−27 prompted us to monitor GD 323 over the last year and finally to obtain a series of six spectra during one night. In addition, the accumulation of a high signal-to-noise ratio spectrum might be especially worthwhile since GD 323 shows the richest hybrid spectrum of the known DAB stars. In this paper we report on these new observations and our extensive efforts to analyze them with theoretical model atmospheres.

2. OBSERVATIONS

An optical spectrum of GD 323 was obtained in 1982 with the Palomar Double CCD Spectrograph by Greenstein (1986). The spectral resolution of this observation is approximately 20 Å. More recently, spectra were obtained with the Boller & Chivens spectrograph at the Steward 2.3 m telescope in 1992 and 1993, as listed in Table 1, all with a spectral resolution of about 7 Å.

[1] Current address: Institut für Theoretische Physik und Sternwarte, Christian-Albrechts-Universität, Olshausenstraße 40, D-24098 Kiel, Germany.
[2] Guest Observer with the *International Ultraviolet Explorer* satellite, which is jointly operated by the US National Aeronautics and Space Administration, the Science Research Council of the UK, and the European Space Agency.
[3] Operated by the Association of Universities for Research in Astronomy, Inc., for the National Aeronautics and Space Administration.

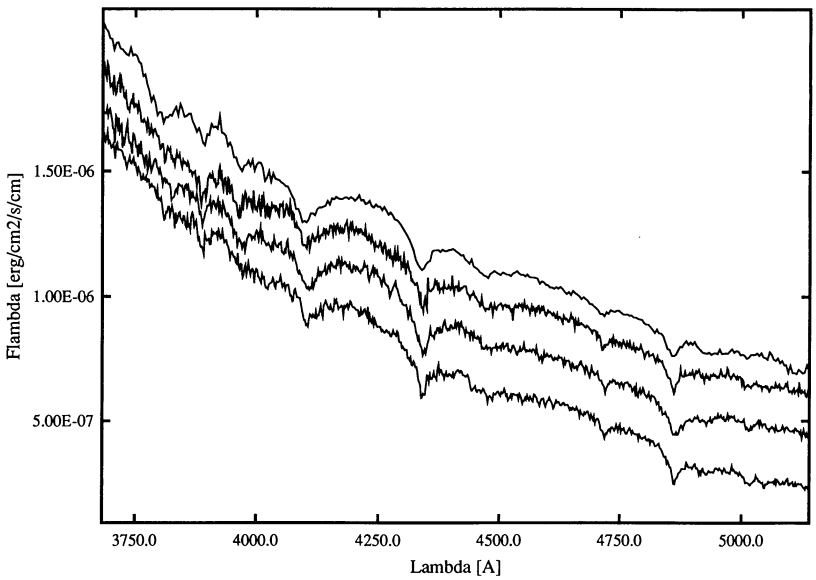

FIG. 1.—Observations of GD 323. From top: 1982 Greenstein (Palomar), 1992 March 25, 1993 March 15 and 1992 June 30. The exact start time and exposure time of the Greenstein spectrum are not available to us. The lower three spectra were all obtained at the Steward 2.3 m telescope. The vertical (flux) scale is correct for the Palomar spectrum; the others have been shifted vertically.

TABLE 1

LOG OF OBSERVATIONS

Date	Start Time (UT)	Time (s)
1992 Mar 25	8:16	600
1992 Jun 30	14:39	900
1993 Mar 15	12:24	600
1993 Mar 31	7:04	600
	7:17	600
	7:29	600
	7:41	600
	9:05	600
	12:05	600

Figure 1 shows the four earlier spectra. Differences between the Steward and Palomar spectra are mostly due to the different resolution, but there are also indications of small differences in the Balmer line profiles. These possible differences—which we cannot judge now to be significant—motivated us to obtain the six spectra shown in Figure 2, taken during the one night (1993 March 31). The flux level in these spectra differs by a few percent, and there are also small shifts in wavelength (less than $\frac{1}{2}$ resolution element); however, the line spectrum does not show any significant variations. We have therefore added all six of the 1993 March 31 spectra (after correcting for the small shifts using cross-correlation techniques) to obtain the top spectrum in Figure 2, with a

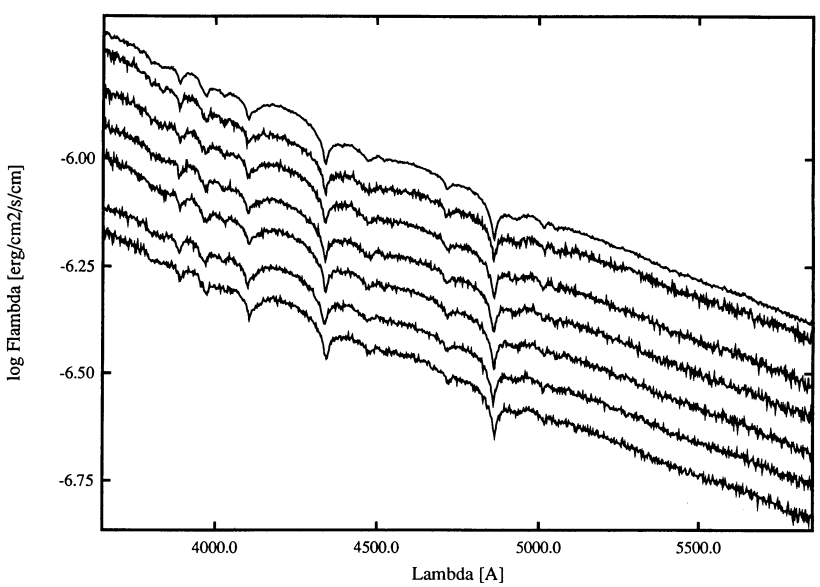

FIG. 2.—Six spectra of GD 323 obtained during one night (1993 March 31) at the Steward 2.3 m telescope. The top spectrum is the combined spectrum on the correct flux scale; the other six below the ordered by time of observation and shifted arbitrarily.

signal-to-noise ratio of about 300. This combined spectrum was used in our analysis of the optical spectrum described below, under the assumption that the spectrum is nonvariable. The spectrum is available in electronic form from the first author to anyone requesting it.

An anonymous referee has requested that we quantify the statement about nonvariability. This is an almost impossible task. As mentioned above, the overall flux level in the different spectra varied (about 10%), and the earlier spectra showed also differences in Balmer line profiles. These differences can easily be explained by different reduction methods and resolutions. With the spectra obtained in the night with identical instrumentation, and after adjusting for a few percent differences in absolute flux levels, the remaining differences are compatible with the noise of the individual spectra. Our conclusion is that all observed differences are compatible with the assumption that the star shows no variability. This does not exclude the possibility of small variations of individual line strengths of the order of 2%–3%, which, however, do not affect our conclusions.

GD 323 has also been observed in the UV with the *IUE* (*International Ultraviolet Explorer*) satellite in the long and short-wavelength *IUE* ranges. This spectrum was already used by LWSW; we have used the SWP 17401 and LWR 13654 spectra taken on 1982 July 11, and corrected them with the latest version of Finley's correction to the absolute energy scale (Finley 1992). With the UV spectra and the absolutely calibrated optical spectra the total energy distribution for GD 323 is well determined between 1200 and 6000 Å.

Although many alternative model explanations for GD 323 were already studied by LWSW, we have repeated most of their analysis with the new, vastly superior observations. A second reason was that we wanted to use a consistent set of model atmospheres, calculated with exactly the same input physics, for the different scenarios.

3. GD 323: A MIXED COMPOSITION SINGLE DAB STAR?

This is of course at first glance the most natural explanation and has been studied extensively by LWSW. We have repeated this study with an extensive grid of model atmospheres newly calculated for this purpose. Effective temperatures range from 20,000 K to 45,000 K, and the He/H ratio was 0.02, 0.1, 1, 10, and 50. For most models log $g = 8$ was used, but some test calculations for other gravities confirm the conclusion that none of these models can explain the observed spectrum of GD 323.

For each abundance series we have first selected the models that reproduce best the overall continuum energy distribution from the UV to the red. For the more hydrogen-rich models this is close to 24,000 K; increasing the helium abundance in the models decreases the slope and higher effective temperatures are necessary. For the He/H = 10 series the best-fitting temperature is 26,000 K, for He/H = 50 it is about 30,000 K, because the continuum distribution is now dominated by the helium.

Figure 3 shows a comparison of the observations with three models that fit the overall flux level in the UV. The second spectrum from top is the observation. The two lower spectra are for $T_{\rm eff} = 24{,}000$ K, He/H = 0.02 and 0.1; the top spectrum is $T_{\rm eff} = 26{,}000$ K and He/H = 10 (all theoretical spectra are arbitrarily shifted). While the weak helium lines in the most helium-poor model fit, because they are not resolved, the stronger helium lines (4471) are much too narrow. In the two lower models the H lines are too strong, while in the upper model the H lines are already too weak and the helium lines too strong.

While the overall level of flux in the UV is reproduced by these models, the slope of the UV continuum is not. Figure 4 shows a typical result for the energy distribution for the He/H = 0.1 series and temperatures between 24,000 and 30,000 K, fitted to the observations in the red part of the optical spectrum. The flux around 2500–3000 Å is always too low in the models, whereas at shorter wavelengths (1200–2000 Å) the model flux is too high. The physical reason behind this is simple: if the optical hydrogen lines are to be reproduced by this type of model, the continuum opacity in the UV is dominated by the Balmer continuum, with strong absorption below the Balmer edge, decreasing strongly toward the far-UV.

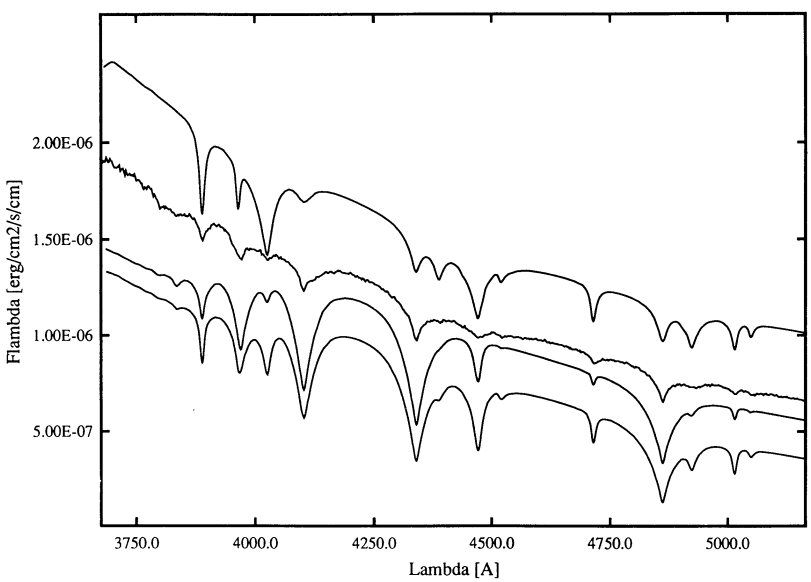

FIG. 3.—Analysis of GD 323 with homogeneous mixed H/He atmospheres. The observation (*second from top*) is compared to two models that reproduce the overall UV flux level (though not the correct shape). *Top*: $T_{\rm eff} = 26{,}000$ K, He/H = 10; *second from bottom*: $T_{\rm eff} = 24{,}000$ K, He/H = 0.02; *bottom*: $T_{\rm eff} = 24{,}000$ K, He/H = 0.1. The surface gravity is log $g = 8.0$ for all models, and the models have been shifted vertically for clarity.

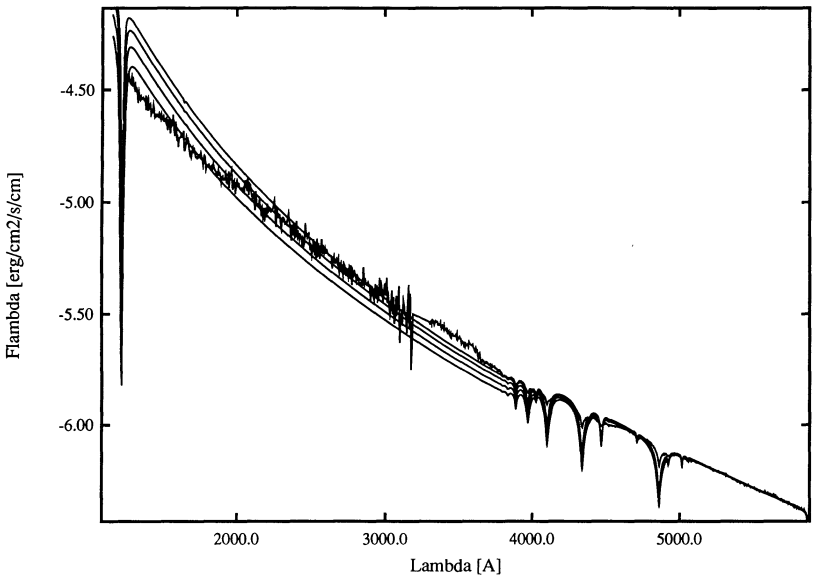

FIG. 4.—Energy distribution for homogeneous models with He/H = 0.1 and effective temperatures from 24,000 to 30,000 K, in increments of 2000 K. All models have been fitted to the observation in the red.

No composition exists which can simultaneously explain the continuum energy distribution, the hydrogen lines, and the helium lines. This result remains true also, if we allow the surface gravity to vary between 7.5 and 8.5. This conclusion was reached already by LWSW; we confirm it with our new models and data.

4. GD 323: A DA + DB COMPOSITE?

This is one of the obvious possibilities discussed and dismissed by LWSW. We have repeated the analysis with the new observations and our new model grids.

Since the number of possible combinations is very large, we have used an "automatic" method to narrow the range of any probable solution. The first step in this procedure was to define observational quantities that should be reproduced by the theoretical model. These consisted of two numbers describing the flux ratios of the far- and near-UV to the optical continuum, and eight equivalent widths of H and/or He features in the optical spectrum. Table 2 gives the adopted values and the definition of the wavelength ranges for the equivalent widths. The "errors" were deliberately chosen larger than necessary in view of the exceptional quality of the spectra—we did not want to miss any possible combination.

In the next step we chose a selection of 75 DA and 144 DB models from our model grids, covering the range of effective temperatures between 13,000 and 45,000 K and surface gravities log g from 7.4 to 8.5.

The automatic procedure then went through the 10,800 possible combinations of DA + DB models, adjusted the fluxes for the different solid angles corresponding to the surface gravities and determined weighted residuals between observed and model features. This constitutes essentially a χ^2 fitting procedure to the 10 features with the $T_{\rm eff}$ and log g of the two components as free parameters.

No combination in this procedure came close to being acceptable; the minimum (reduced) χ^2 obtained was in the range 6–10. Given the fact that the errors assumed are already unrealistically high this definitely excludes any composite explanation with parameters in the considered range.

Closer inspection of the results and a detailed comparison of composite models with the observations allows the following statements:

1. The slope (UV/optical) of the continuum can be explained either by a hydrogen model with $T_{\rm eff} \approx 24{,}000$ K, or by a helium model with $T_{\rm eff} \approx 30{,}000$ K. None of the "best" 1000 combinations in our procedure includes a hydrogen model with $T_{\rm eff} < 25{,}000$ K. The reason is simple: in order to reproduce the slope, the DB has to have $T_{\rm eff} > 30{,}000$ K, which leads to too strong He lines that are not sufficiently diluted by the optical continuum of the DA.

2. In the intermediate range, with both components having $T_{\rm eff}$ between 24,000 and 30,000 K, it is possible approximately to reproduce the average continuum slopes and the helium lines. The hydrogen lines are always much too strong, however, and closer inspection shows that the shape of the UV spectrum is not well reproduced. The observed spectrum shows very little curvature if the logarithmic flux is used. The theoretical

TABLE 2

FEATURES USED FOR PRELIMINARY SELECTION OF DA + DB COMPOSITES[a]

Feature	Value	Error
log (F_{1500}/F_{5500}) ...	1.65	0.05
log (F_{2500}/F_{5500}) ...	1.09	0.07
λλ 3865–3925	1.35	0.34
λλ 3925–4000	1.83	0.46
λλ 400–4045	0.42	0.10
λλ 4050–4180	3.87	0.76
λλ 4250–4420	8.03	1.25
λλ 4420–4540	2.51	0.50
λλ 4680–4770	1.38	0.34
λλ 4790–4975	9.89	1.25
λλ 4895–4965	0.70	0.16
λλ 4980–5030	0.82	0.16

[a] The first two numbers in the value column are flux ratios, all other values are equivalent widths.

models, on the other hand, are invariably too low around 2500 Å and too high around 1350 Å, if they fit on average.

3. By far the best formal fits are obtained with hot (> 30,000 K) hydrogen models and cool (15,000–16,000 K) helium models. The hydrogen lines can be fitted quite well. The far-UV flux is too high, however, and the helium lines are too narrow, even if the equivalent widths are correct.

Figure 5 shows as an example the optical spectrum for two of the best combinations, highlighting the points made above.

5. INHOMOGENEOUS SURFACE COMPOSITION: THE SPOT MODEL

While the concept of inhomogeneous surface distribution of chemical elements is familiar in the context of peculiar A stars, it has been applied in the field of white dwarfs only very recently. Achilleos et al. (1992) used it to explain the variable spectrum of the peculiar DBA magnetic white dwarf Feige 7, and Beauchamp et al. (1993) proposed the concept for the object of this study, GD 323. The theoretical background for this assumption is the idea that the temperature of GD 323 puts it close to the limit, where the convection zone in the deeper helium layer extends upward, mixing—perhaps not in a spherically symmetric manner at first—with the upper hydrogen layer (Fontaine & Wesemael 1987).

The fact that the spectrum does not seem to vary significantly on time scales of hours, months, and years makes this explanation somewhat unlikely from the beginning, although it cannot be excluded if the rotation rate is extremely slow, the viewing angle is unfortunate, or we accidentally happened to observe always at the same phase.

Since nothing can be inferred about the distribution or the shape of the spots, we use in the exploration an even simpler physical model than Beauchamp et al. (1993). We assume that a fraction of the surface is covered by pure hydrogen and the remaining part by pure helium, both of which emit spectra like a simple DA or DB. We assume that there is no horizontal pressure gradient, and thus the surface gravities are equal (= 8.00) for both models. It is unlikely that the effective temperatures can differ by more than a few thousand K, but we have nevertheless searched our entire grid of log $g = 8.0$ models with 20 different values of the hydrogen fraction between 0.0 and 1.0. For a preliminary selection of possible models we used the same observationally defined features used for the analysis in the previous chapter. Since we use the same set of pure DA and DB models as for the analysis of the binary model, it might be argued that this is only a subset of the previous analysis. That is, however, not completely true. The first difference is that with the spot model, we have the fraction of DA versus DB as a completely free parameter, whereas in the case of the binary model the choice is limited by the range of reasonable surface gravities (and thus radii) of the two stars. On the other hand, the effective temperatures of the stars could be treated as free parameters in the binary models, whereas in the spot model we would not expect the temperatures of different regions on the same star to differ by more than a few thousand degrees.

The combinations that give the best overall fit to slopes and equivalent widths are again combinations of a hot DA with a cool DB. However, the fits to the line profiles are completely unsatisfactory in a manner similar to the DA + DB binary combination: while the hydrogen lines can be fitted reasonably well, the helium lines are too narrow. Combinations with hotter DB stars, which would fit the He line profiles better, are excluded because the energy distribution cannot be fitted. The same is true if we confine the search to models that differ by no more than 5000 K, which seems justifiable on physical grounds: none of the combinations that give the correct energy flux at the shortest wavelengths can fit even the equivalent widths. Figure 6 shows two examples for models of this class. The top model is a combination of a 37,500 K DA (15%) and a cool DB (15,000 K, 85%), which fits the UV flux level (but not the slope!). The bottom model is one of the best fits where the temperature difference is restricted to 5000 K. In this model the UV flux is far too high.

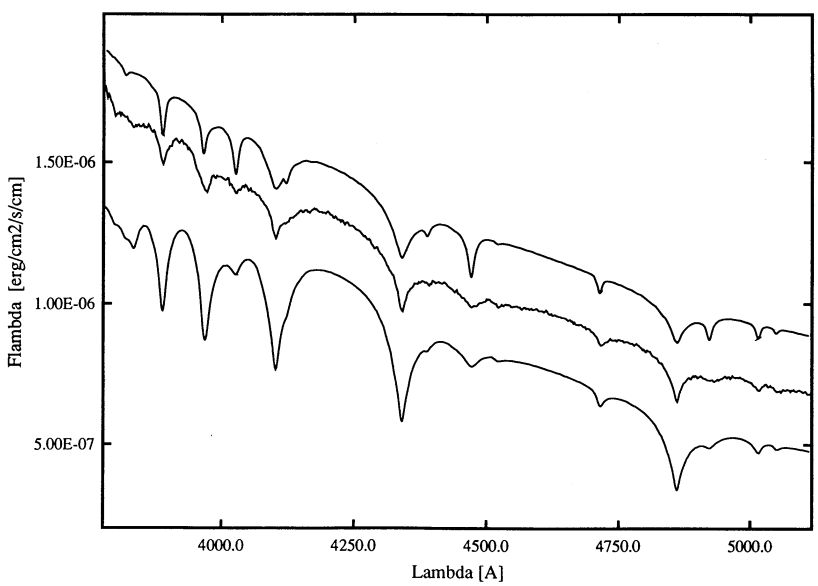

FIG. 5.—Analysis with composite DA + DB models. The observed spectrum (*middle*) is compared to two combinations with the correct UV overall flux. *Top*: DA with $T_{\rm eff} = 32{,}500$ K, log $g = 8.5$ and DB with $T_{\rm eff} = 15{,}000$ K, log $g = 7.4$. *Bottom*: DA with $T_{\rm eff} = 25{,}000$ K, log $g = 7.5$ and DB with $T_{\rm eff} = 25{,}000$ K, log $g = 8.4$. Theoretical models are shifted vertically.

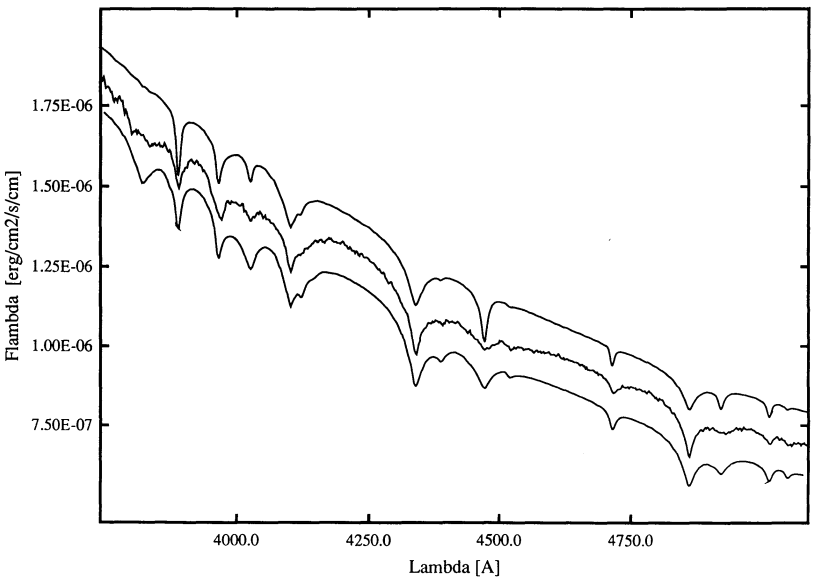

FIG. 6.—Analysis with "spot" model, simulated with a combination of pure DA and DB models representing a fraction of the stellar surface. *Middle*: observed spectrum; *Top*: DA, $T_{\rm eff}$ = 37,500 K, surface fraction 15%, DB, $T_{\rm eff}$ = 15,000 K, surface fraction 85%. *Bottom*: DA, $T_{\rm eff}$ = 37,500 K, surface fraction 55% and DB, $T_{\rm eff}$ = 34,000 K, surface fraction 45%. Both model combinations produce the correct overall UV flux, but not the correct slope.

6. A STRATIFIED H/He ATMOSPHERE?

The last model we have explored is that of a stratified atmosphere with a thin hydrogen layer floating on top of the underlying helium atmosphere. In some sense this would be the most appealing solution, since we expect the separation of H and He due to gravitational separation on a very short time scale in hot DA white dwarfs, if there are no counteracting processes like convection (Schatzman 1949). Such models have been calculated in the meantime and applied in preliminary analyses to GD 323 (Koester 1989, 1991). Our models used here are basically the same as described in Koester (1991) with one exception: the diffusion equation, which describes the structure of the transition zone between pure H and pure He layers, is solved numerically within the atmosphere model code, to allow for variable ionization within the transition zone. The model grid extends from 25,000 to 33,000 K in effective temperature; the parameter that is used to describe the thickness of the hydrogen layer is log $Pg0$, the gas pressure at the layer where the number abundances of H and He are equal. It is directly related to the total hydrogen mass, which is now also obtained from the numerical solution of the diffusion equation within the atmosphere, thus taking into account any homogeneously mixed convection zones. The hydrogen content in the envelope below the bottom of the calculated atmosphere is estimated from the simple analytic solution of the diffusion equation for small H fractions.

If all layers are in radiative equilibrium or if the convection zone is completely within the atmosphere, this calculation of the total hydrogen mass is quite accurate. However, in the case of convection zones extending to the bottom of the calculated atmosphere, it gives only a lower limit to the total hydrogen mass, because the large additional amount of hydrogen could be hidden in the helium-rich convective envelope. This is, however, not the case in the models giving the best fits, which at most have a very thin convective layer in the region of almost pure helium, without any influence on the element stratification.

Since the number of free parameters is more limited in this case, we have employed a direct χ^2 fitting technique independently to the whole energy distribution from UV to the red as well as to the optical spectrum alone. The best fits were obtained in both cases for effective temperatures near 28,750 K ($\pm$1000 K) and log $Pg0 = 5.15$ ($\pm$0.10). This value of the H layer parameter corresponds to a very thin hydrogen layer with $M_{\rm H} = 1.05 \pm 0.3 \times 10^{-17}\, M_\odot$.

These models can reproduce the energy distribution—even the UV slope—quite well, as shown in Figure 7. This is in fact the only class of models that we have studied, which shows the observed very small curvature in the logarithmic plot. The fit to the line spectrum is shown in Figure 8 with a model at $T_{\rm eff}$ = 28,750 K and log $Pg0 = 5.2$, close to the nominally best fit found. The result is very similar (except for a slightly higher temperature) to the preliminary result in Koester (1991) based on older observations, and has similar shortcomings. The helium lines are reproduced fairly well, as is the overall strength of the Balmer lines. However, closer inspection shows as already found by Koester (1991) that the Balmer line profiles are too narrow and the wings are too weak. We have confirmed again that this result is not changed when allowing higher surface gravities in the models.

7. DISCUSSION AND CONCLUSIONS

In this study we have explored four different classes of models to explain the almost unique spectrum of the hybrid star GD 323: a mixed composition H/He atmosphere, a binary DA + DB composite, a simple "spot" model, and a stratified H/He atmosphere in diffusion equilibrium. In spite of a very extensive search with large model grids we have found no completely satisfactory solution. The first three possibilities can almost certainly be excluded for similar reasons: it is impossible to explain the energy distribution, which is well determined from the far-UV to the red optical spectrum, *and* the H/He line spectrum, with a consistent model. In particular, none of the models predicts a UV energy distribution with the small curvature between 1200 and 3000 Å that is observed. In all models of these classes the continuum opacity in this range is dominated

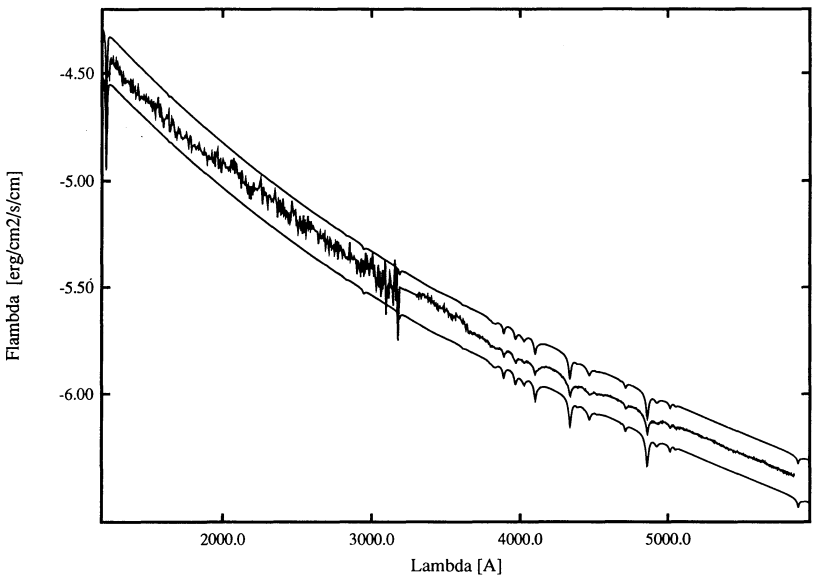

FIG. 7.—Analysis with stratified models. Observed energy distribution from UV to red (*middle*) and two stratified models with $T_{\rm eff}$ = 28,000 K (*top*) and 29,000 K (*bottom*). $M_{\rm H}$ is 2.45 × 10^{-17} $M_{\odot}$ in both models.

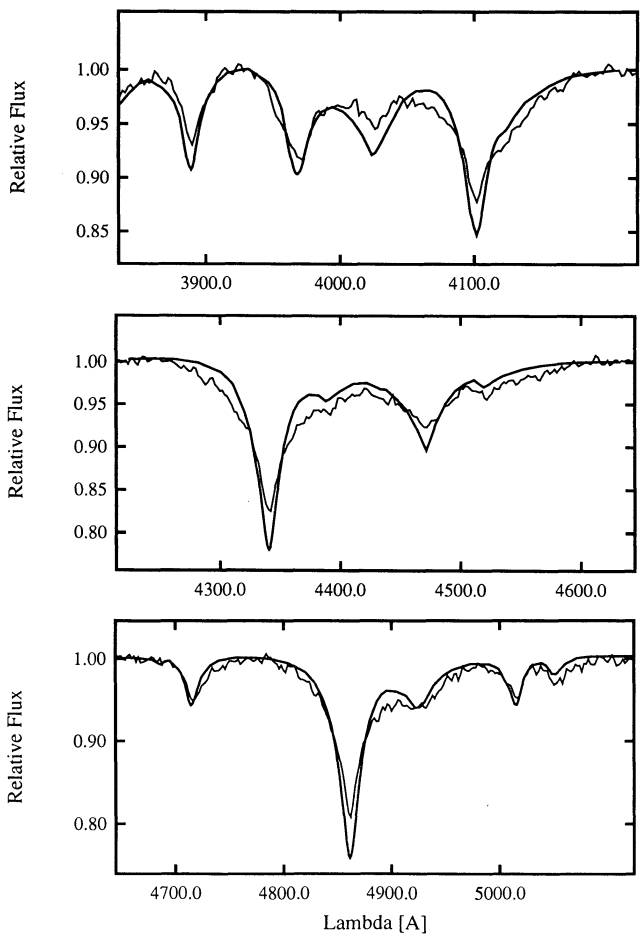

FIG. 8.—Fit of the optical spectrum with stratified models. The observed spectrum is the thin line. It is compared to a theoretical model (*thick line*) with $T_{\rm eff}$ = 28,750 K and $M_{\rm H}$ = 1.05 × 10^{-17} $M_{\odot}$. The continuum on both sides of each individual panel has been normalized to 1.

by hydrogen, with large absorption just shortward of the Balmer jump, steeply decreasing toward the far-UV. This invariably leads in the models considered to a flux distribution rising much steeper toward the far-UV than is observed. Turning this argument around, we conclude that the UV opacity most likely is dominated by helium, which, however, at least in the first three scenarios is incompatible with the line spectrum.

The closest match to the observations is obtained by a stratified atmosphere model. This model can explain the energy distribution *and* the helium line spectrum; it fails for the hydrogen line wings. With the new, extremely high S/N spectra it is apparent that hydrogen line absorption is missing from regions with higher pressure, since in the stratified models hydrogen is confined to the outer regions.

Given the result that among the unsatisfactory results the stratified models come closest to the reality, we might ask if further changes to the models might be demanded to improve the situation. All models used have been calculated with state of the art model atmosphere techniques using the "correct" input physics according to the best of our knowledge. This includes H and He line broadening theories, the occupation probability formalism after Hummer & Mihalas (1988), and the diffusion equations including variable ionization. We do not currently see any possibility of improvements or reasons for artificial manipulations in these areas, although it cannot be excluded that processes in addition to simple gravitational separation—e.g., a very small unobservable stellar wind with its associated velocity field in deeper layers—might alter the element distribution. The single one physical input that is subject to much larger uncertainties is the treatment of convection.

Our standard set of models is calculated with the usual mixing length approximation and a ratio of mixing length to pressure scale height of 1. With this value, the best-fitting stratified model has a convection zone between Rosseland optical depths of 4–50 and the model is radiative again to the bottom of the calculated atmosphere at optical depth 1750. In the

larger context of the evolution of white dwarf spectral types this is somewhat unsatisfactory, because it would mean that the total hydrogen mass is only a few times $10^{-17}\ M_{\odot}$, and has probably been that small in the precursor stages of GD 323. Such a star would show He lines also at higher temperatures in earlier phases, which is at odds with our current empirical knowledge of the "DB gap" (Liebert, Fontaine, & Wesemael 1987; Liebert 1991), i.e., the fact that no stars with He lines were observed in the temperature range 30,000–45,000 K. This fact has only very recently been challenged with the discovery of the hybrid H/He object HS 0209+0832 at a probable temperature of 36,000 K (Jordan et al. 1993). While this object is best fit with a homogeneous H/He atmosphere, a final conclusion has to wait for a thorough analysis of other possibilities (e.g., a binary scenario) comparable to this study.

Returning to the object of the present study, within possible evolutionary scenarios for white dwarf envelopes it would be more satisfactory to find a model that represents the observed spectrum of GD 323, but with a convection zone extending to the bottom of the atmosphere and beyond, which could easily contain the remainder of the perhaps $10^{-15}\ M_{\odot}$ hydrogen that is usually invoked to explain the DB gap and the onset of the DB sequence (through convective mixing of the hydrogen) around or slightly below 30,000 K (Liebert 1991; MacDonald & Vennes 1991). Because of our limited knowledge about convection we have conducted one experiment with artificially increased convective efficiency by setting the mixing length parameter to 3. In this case the convection zone is indeed much more extended as expected, reaching the bottom of our calculated atmosphere. The hydrogen number abundance remains constant throughout the convection zone at about 3×10^{-3}, and the total hydrogen mass as calculated by our program increases to approximately $10^{-16}\ M_{\odot}$. This is of course a lower limit in this case, since the depth of the convection zone is not given by our atmosphere calculation, and even at this small abundance the total H mass in the deeper layers can be significant.

Unfortunately this experiment does not solve the problem of the observed Balmer line wings, because the top of the convection zone remains at the same location, where the hydrogen abundance is already too low to contribute significantly to the lines. If we still want to favor stratified atmospheres as the most promising hypothesis, this indicates, on the other hand, that any changes in input physics that will come closer to reproducing the observations will have to be effective at the top of the convection zone. While it is possible to speculate about deviations from the classical mixing length approximation—for example, overshooting and turbulent mixing at the upper limit of the zone that changes the structure of the composition gradient—we feel that this would go far beyond the scope of the present study.

In summary: by excluding many alternatives as highly unlikely, we have demonstrated that the most promising explanation remaining is indeed in terms of stratified atmospheres. However, before this can be finally accepted we will need a better understanding of the interplay of convection with diffusion and the combined effect of the element stratification.

We thank Jesse L. Greenstein for providing his early CCD spectrum of GD 323, and Mike Fulbright for help with the observations and reductions. This work was supported in part by grants AST 91-45162 (J. L.) and AST 90-18244 (D. K.) from the National Science Foundation.

REFERENCES

Achilleos, N., Wickramasinghe, D. T., Liebert, J., Saffer, R. A., & Grauer, A. D. 1992, ApJ, 396, 273
Beauchamp, A., Wesemael, F., Fontaine, G., & Bergeron. P. 1993, in White Dwarfs: Advances in Observation and Theory, ed. M. Barstow (Dordrecht: Kluwer), in press
Finley, D. 1992, private communication
Fontaine, G., & Wesemael, F. 1987, in IAU Colloq. 95, The Second Conference on Faint Blue Stars, ed. A. G. Davis Philip, D. S. Hayes, & J. W. Liebert (Schenectady: L. Davis Press), 319
Greenstein, J. L. G. 1969, ApJ, 158, 281
———. 1986, ApJ, 304, 334
Holberg, J. B., Kidder, K. M., & Wesemael, F. 1990, ApJ, 365, L77
Hummer, D. G., & Mihalas, D. 1988, ApJ, 331, 794
Jordan, S., Heber, U., Engels, D., & Koester, D. 1993, A&A, in press
Jordan, S., & Koester, D. 1986, A&AS, 65, 367
Kidder, K. M., Holberg, J. B., Barstow, M. A., Tweedy, R. W., & Wesemael, F. 1992, ApJ, 394, 288
Koester, D. 1989, in IAU Colloq. 114, White Dwarfs, ed. G. Wegner (Berlin: Springer), 206
———. 1991, in IAU Sympos. 145, Evolution of Stars: The Photospheric Abundance Connection, ed. G Michaud & A. Tutukov (Dordrecht: Kluwer), 435
Liebert, J. 1991, in IAU Symp. 145, Evolution of Stars: The Photospheric Abundance Connection, ed. G. Michaud & A. Tutukov (Dordrecht: Kluwer), 411
Liebert, J., Fontaine, G., & Wesemael, F. 1987, Mem. Soc. Astron. Italiana, 58, 17
Leibert, J., Wesemael, F., Sion, E. M., & Wegner, G. 1984, ApJ, 277, 692 (LWSW)
MacDonald, J., & Vennes, S. 1991, ApJ, 371, 719
Oke, J. B., Weidemann, V., & Koester, D. 1984, ApJ, 281, 276
Price, C. W., & Shipman, H. L. 1985, ApJ, 295, 561
Robinson, E. L., & Winget, D. E. 1983, PASP, 95, 386
Schatzman, E. 1949, Publ. Copenhagen Obs. No. 149
Vennes, S., Fontaine, G., & Wesemael, F. 1989, in IAU Colloq. 114, White Dwarfs, ed. G. Wegner (Berlin: Springer), 368
Vennes, S., & Fontaine, G. 1992, ApJ, 401, 288
Wesemael, F., et al. 1993, in White Dwarfs: Advances in Observed and Theory, ed. M. Barstow (Dordrecht: Kluwer), in press